Waste Management 169 (2023) 267–275

Contents lists available at ScienceDirect

Waste Management

journal homepage: www.elsevier.com/locate/wasman

Co-hydrothermal carbonization of swine manure and lignocellulosic waste: A new strategy for the integral valorization of biomass wastes

R.P. Ipiales [a,b], A.F. Mohedano [a,*], E. Diaz-Portuondo [b], E. Diaz [a], M.A. de la Rubia [a]

[a] Chemical Engineering Department, Universidad Autónoma de Madrid, 28049 Madrid, Spain
[b] Arquimea-Agrotech, 28400 Collado Villalba, Madrid, Spain

ARTICLE INFO

Keywords:
Anaerobic digestion
Co-hydrothermal carbonization
Energy recovery
Garden and park waste
Process water valorization
Swine manure

ABSTRACT

Co-hydrothermal carbonization (co-HTC) is a promising strategy to improve hydrothermal carbonization (HTC) of low-quality wastes. HTC of swine manure (SM), with high N (2.9 wt%), S (0.7 wt%) and ash (22.6 wt%) contents, as well as low C (35.6 wt%) and higher heating value (HHV; 14.3 MJ kg^{-1}), resulted in a hydrochar with unsuitable characteristics as a solid fuel. Co-HTC of SM and garden and park waste (GPW) improved hydrochar properties (C content (43 – 48 wt%) and HHV (18 – 20 MJ kg^{-1}), and decreased N (~2 wt%), S (<0.3 wt%) and ash (<15 wt%) content. A high GPW ratio (>50 wt%) during co-HTC resulted in a hydrochar similar to that obtained from GPW. The co-HTC increased nutrient migration to the process water, which allowed the precipitation of salt with high P (7.8 wt%) and negligible heavy metal content. Anaerobic digestion of co-HTC process water allowed high organic matter removal (up to 65%), and methane production (315 – 325 mL CH_4 $g^{-1}COD_{added}$). Gross energy recovery by HTC and anaerobic digestion was 5 – 6-fold higher than anaerobic treatment of feedstocks. Therefore, co-HTC of SM and GPW with a ratio > 50% GPW proved to be a suitable approach to valorize and manage SM and obtain value-added products (hydrochar, mineral fertilizer and methane).

1. Introduction

Animal manure is one of the main wastes generated in the EU (excluding mineral and construction waste). Although livestock populations have experienced a slight reduction (≈ 2.1%) in the EU between 2001 and 2021 (EUROSTAT, 2020), livestock waste (≈ 22 Mt d.b.) and greenhouse gas emissions (GHG, ≈ 520 Mt $CO_{2equivalent}$) ascribed to this sector, have not undergone significant changes (EEA, 2020). Traditionally, animal manure has been directly applied on agricultural soils as organic fertilizer, which favors plant growth, because of the contribution of nutrients and organic matter (Köninger et al., 2021), but causes serious environmental problems associated with ammonia nitrogen content and the introduction of inhibitory elements such as heavy metals, antibiotics, and pathogens (Weiss and Leip, 2012).

Hydrothermal carbonization (HTC) is a promising and low-cost alternative to transform biomass waste with high moisture content into a carbonaceous solid, called hydrochar, with improved characteristics with respect to the initial feedstock, a liquid fraction with high organic and nutrient content, called process water, and a minimal gas fraction (Villamil et al., 2019). Hydrochar has a higher energy densification and better combustion behavior than the feedstock (Benavente et al., 2015; Lang et al., 2019c), but usually the feedstock quality is a key factor to obtain a suitable hydrochar as solid biofuel (Bardhan et al., 2021), soil amendment (Jin et al., 2019) or activated carbon precursor (Diaz et al., 2019). Animal manure (dairy, poultry and swine manure) is characterized by high N (2 – 6 wt%), S (0.5 –3 wt%) and ash (15 – 30 wt%) content, moderate C content (30 – 40 wt%) and relatively low higher heating value (HHV; 13 – 18 MJ kg^{-1}) (Lang et al., 2018; Mariuzza et al., 2022; Song et al., 2020), resulting in a low-quality hydrochar with characteristics unsuitable for using as a solid biofuel according to ISO/TS 17225–8 (2016) (N > 3 wt%, S > 0.5 wt%, ash > 10 wt%, volatile matter (VM) > 75 wt% and HHV < 17 MJ kg^{-1}). Previous studies reported that hydrochar obtained from animal manure showed an increase in N (0.5 – 3 wt%) and ash (5 – 15 wt%) content, low hydrochar mass yield (Y_{HC}; 40 – 55 wt%) and energy recovery (E_{yield}; 40 – 65%) (Lang et al., 2019a; Qaramaleki et al., 2020). Likewise, high ash content in hydrochar reduces combustion stability and increases ignition and burning temperature, resulting in incomplete combustion and high NO_X and SO_2 emissions (Owsianiak et al., 2016; Ro et al., 2019). For these reasons, animal manure HTC is not suitable to properly

* Corresponding author.
E-mail address: angelf.mohedano@uam.es (A.F. Mohedano).

https://doi.org/10.1016/j.wasman.2023.07.018
Received 11 April 2023; Received in revised form 11 July 2023; Accepted 12 July 2023
Available online 22 July 2023

manage these wastes. Several pretreatments and post-treatments have been described in the literature to improve the quality of hydrochar, such as HTC-assisted by catalyst (acid or salt) (Kambo and Dutta, 2015; Lang et al., 2019c), hydrochar washing (Ipiales et al., 2023; Pecchi et al., 2022) or hydrochar blending with coal for energy purposes (Zhang et al., 2020). However, these practices generate other uncertainties, such as the expenses of a catalyst or washing solvent (commonly an inorganic acid), which incurs in an additional cost, requires expensive corrosion-resistant equipment, and generates a more complex liquid effluent to manage (Ipiales et al., 2023). In the case of co-combustion, the large energy densification gap means that hydrochar promotes fast and incomplete combustion of coal, resulting in low energy efficiencies (Gao et al., 2019).

Co-hydrothermal carbonization (co-HTC) is a new trend with positive results, which seeks synergistic interaction between two feedstocks during hydrothermal process. Co-HTC can improve the characteristics of hydrochar by increasing the C content, and HHV, improving combustion properties (Bardhan et al., 2021; Saba et al., 2019), and decreasing the N, S, and ash content of hydrochar, as well as the presence of heavy metals and polycyclic aromatic hydrocarbons (Hadroug et al., 2021; Lang et al., 2019b; Mariuzza et al., 2022). Most studies on co-HTC have focused on bettering the low quality of hydrochar from animal manure, sewage sludge or microalgae by blending with lignocellulosic biomass. Lignocellulosic biomass provides high C (40 – 55 wt%) and HHV (17 – 24 MJ kg^{-1}) and low N (<2 wt%), S (<1 wt%) and ash (<15 wt%) (Cheng et al., 2020; Lynam et al., 2015). In this case, the mixture of low moisture but high-quality characteristics waste (such as lignocellulosic biomass) with animal manure characterized by high moisture, as well as N, S and ash content can have a positive effect on the characteristics of the resulting hydrochar. A positive effect of co-HTC is the increase of decarboxylation and dehydration rate, reduction of H/C and O/C ratios and promotion of carbonization degree (Bardhan et al., 2021), as well as improvement of N migration and mineralization (Wang et al., 2022), and thermal stability of hydrochar (Mariuzza et al., 2022). Also, co-HTC changes the process water characteristics, enhancing C/N ratio, phosphorus migration, and bioavailability of short-chain organic compounds for biological valorization (Sharma et al., 2022; Wang et al., 2022). Furthermore, co-HTC enables the valorization of unattractive or unsuitable waste materials that would not be suitable for standalone HTC using lignocellulosic biomass (Bardhan et al., 2021; Mariuzza et al., 2022), which requires water for the process. This synergistic approach between different waste streams results in the production of higher-quality products while also saving water and enhancing the overall HTC process (Inkoua et al., 2023). This advancement makes co-HTC an attractive, suitable, and effective tool for waste valorization, searching of harnessing different streams with specific characteristics suitable for each respective waste. Negative effects of co-HTC could be related to the heterogeneity of the waste reducing the quality of the hydrochar, the lack of reaction and transformation mechanism of organic compounds understanding and, the generation of recalcitrant compounds, which need a proper management fraction to mitigate the pollutant and negative environmental impacts.

Therefore, co-HTC studies have focused on studying mainly the characteristics of the hydrochar, so it is required to deepen in less studied topics such as nutrient recovery, anaerobic biodegradability of process water, as well as energy recovery through the application of mass and energy balances. In this regard, the study focuses on studying the co-HTC of swine manure (SM) and garden and park waste (GPW) yielding a high quality hydrochar according to ISO/TS 17225–8. The material and energy valorization of the products obtained in the hydrothermal stage, the valorization of the process water by anaerobic digestion (AD), and the recovery of P are evaluated, in an approach to the circular economy framework.

2. Materials and methods

2.1. Feedstock origin

The SM was collected from an intensive swine farm located in Durueloo (Avila, Spain). The GPW was collected at the Migas Calientes composting plant located in Madrid (Spain). The SM was stored at −20 °C, while GPW was stored in closed containers at room temperature. The SM was used without any previous pretreatment, while the GPW was ground and sieved to reduce and homogenize the particle size (< 3 mm). The main characteristics of the raw materials are shown in Table 1 (mean of 3 determinations with standard deviations in brackets).

2.2. HTC experiments

The HTC experiments were conducted in a 4 L ZipperClave® pressure vessel electrically heated at 180 °C for 1 h, with a heating rate of 3 °C min^{-1}. The biomass:water ratio was fixed in 20:80 by weight in all the cases. Samples of 1.5 kg were treated in each HTC and co-HTC runs. In co-HTC experiments, SM:GPW mixtures were treated at 3:1, 1:1 and 1:3 ratios (dry basis). After reaction, the reactor was cooled to room temperature with tap water using an internal cooling loop. The reaction mixture (hydrochar and process water) was separated by centrifugation at 8000 rpm for 10 min (Orto Alresa centrifuge; Madrid-Spain) and vacuum filtration (0.45 μm). The wet hydrochar was dried at 105 °C, ground and sieved (<250 μm) before analysis. The process water was stored at 4 °C for use as a substrate for phosphorus recovery (Section 2.4) and anaerobic digestion (Section 2.5) tests. Hydrochar and process water were labeled as HC or PW, respectively, followed by the feedstock used (i.e., HC-SM, HC-GPW), or the ratio of each waste (HC-3:1, HC-1:1 and HC-1:3). HTC experiments were performed in duplicate.

2.3. Characterization of feedstocks and HTC products

Proximate (volatile matter (VM), fixed carbon (FC) and ash) and ultimate (C, H, N, and S) analysis of feedstocks and hydrochars were

Table 1
Main characteristics of swine manure and garden and park waste in dry basis (wt.%).

	SM	GPW	Mineral metals (g kg^{-1})			Heavy metals (mg kg^{-1})		
				SM	GPW		SM	GPW
TS (%)	5.5 (0.2)	96.3 (0.1)	**Al**	1.4 (0.1)	0.1 (0.0)	**Cr**	9.8 (0.2)	1.4 (0.1)
VM (%)	63.4 (0.4)	74.6 (0.5)	**Ca**	31.2 (1.6)	10.1 (0.2)	**Cu**	137.1 (4.1)	2.5 (0.1)
FC (%)	13.0 (0.4)	18.4 (0.4)	**K**	35.4 (0.8)	4.9 (0.1)	**Ni**	4.1 (0.1)	0.3 (0.0)
Ash (%)	23.6 (0.3)	5.1 (0.3)	**Mg**	13.1 (0.7)	0.8 (0.1)	**Pb**	3.6 (0.1)	0.4 (0.0)
C (%)	35.6 (0.2)	47.2 (0.3)	**Na**	10.2 (0.5)	0.1 (0.0)	**Zn**	256.2 (0.5)	20.1 (0.3)
H (%)	4.8 (0.2)	6.1 (0.1)	**P**	30.7 (0.6)	0.9 (0.1)			
N (%)	2.9 (0.1)	1.3 (0.1)						
S (%)	0.7 (0.1)	0.4 (0.1)						
O (%)	32.5 (0.3)	40.6 (0.1)						
HHV (MJ kg^{-1})	13.5(0.3)	18.4 (0.2)						

Oxygen (O) content were calculated by difference (O = 100 − C − H − N − S–ash (%)).

performed in a Discovery SDT thermogravimetric analyzer (TG 209, F3, Netzsch; Selb, Germany) according to ASTM-D7582 (ASTM, 2015) and CHNS analyzer (LECO CHNS-932; Geleen, Netherlands), respectively. Metal composition (mineral and heavy metals) was measured by inductively coupled plasma atomic emission spectroscopy (ICP-OES) using an Elan 6000 Sciex instrument (Perkin Elmer; Santa Clara, United States).

Process waters were characterized by pH (Crison 20 Basic pH-metre), total solids (TS), and volatile solids (VS) according to standard methods 2540B and 2540E, respectively (APHA, 2005). Total chemical oxygen demand (TCOD), and soluble COD (SCOD) were determined according to Raposo et al. (2008) and 5220D (APHA, 2005), respectively. Total organic carbon (TOC) was determined using a TOC–VCPN (Shimadzu; Kyoto, Japan) analyzer. Volatile fatty acids (VFA) were determined by a gas chromatography instrument (Varian 430-GC; Markham, Canada), equipped with a flame ionization detector (FID) and a capillary column packed (nitroterephthalic acid-modified polyethylene glycol (De la Rubia et al., 2018b). Total Kjeldahl nitrogen (TKN) and total ammonia nitrogen (TAN) were determined by method 4500D and 4500E, respectively, (APHA, 2005). Organic nitrogen (N-Org.) was determined by difference between TKN and TAN. PO_4-P was analyzed photometrically using a Hach Lange (Spectrophotometer DR3900; Düsseldorf, Germany) by LCK350 cuvette test.

2.4. Phosphorus recovery

A sample of 250 mL of process water (PW-1:3) was used for phosphorus recovery (PR) by chemical precipitation. To promote struvite precipitation, $Mg(OH)_2$ solution was added to obtain a 1:1.3:1 M ratio of NH_4:Mg:PO_4 (Weidelener et al., 2008). The mixture was neutralized with NaOH (2 M) at pH 9 while stirring for 20 min at 300 rpm. The precipitated solid was separated by filtration (0.45 μm), dried in an oven at 105 °C during 24 h. Solid was characterized by ICP-OES and total reflection X-ray fluorescence (TXRF; Hertogenbosch Netherlands) spectroscopy on an Extra-II Rich & Seifert spectrometer equipped with a Si–Li detector, to identify the mineral and heavy metals content, and the surface properties, respectively.

2.5. Anaerobic digestion assays

Anaerobic digestion assays were performed in 120 mL glass serum flasks, with an inoculum concentration of 15 g VS L^{-1} and an inoculum-to-substrate ratio (ISR) of 2 on a VS basis. Granular anaerobic sludge from a brewery wastewater treatment plant was used as inoculum and showed the following characteristics: 37.4 (1.1) g TS L^{-1}, 33.2 (1.0) g SV L^{-1}, and 47.4 (1.4) g COD L^{-1}. A basal medium with macro- and micro-nutrients (Villamil et al., 2017), was added to each vial and was filled up to 60 mL (workload) with deionized water, process water and inoculum. The vials were closed with rubber stoppers and metallic crimps, were flushed with N_2 for 2 min (to ensure anaerobic conditions) and kept in a thermostatic water-bath at a mesophilic temperature of 35 (1 °C), with shaking at 120 rpm. AD experiments were monitored using 10 vials (for each substrate): 3 for biogas measurements (volume and composition), and the other 7 were sacrificed to monitor anaerobic digestion variables such as pH, TAN, SCOD, TOC and VFA. Substrate-free samples as well as strach-fed control samples (soluble potato strach; Panreac) were used to establish the background biogas level of the inoculum, and to confirm inoculum activity, respectively, both in triplicate. The control produced 350 (10) mL STP CH_4 g^{-1} COD_{added}. The biogas composition (H_2, CO_2, CH_4 and H_2S) were measured by a gas chromatograph (Thermo Scientific Trace 1300; Villebon, France) equipped with a thermal conductivity detector (TCD) using a 8 ft × 1/8 in SS column packed with HayeSep Q 80/100 mesh (De la Rubia et al., 2018a).

2.6. Mass and energy balances

The HC mass yield (Y_{HC}) was calculated as the ratio of weight of hydrochar recovered (W_{HC}) to the weight of feedstock ($W_{Feedstock}$), on dry basis (Eq. (1). The process water yield (Y_{PW}) was calculated as the ratio of the total solids in the PW (TS_{PW}) and volume (V_{PW}) to that in the feedstock ($W_{Feedstock}$) on a dry basis (Eq. (2).

$$Y_{HC}(\%) = \frac{W_{HC}}{W_{Feedstock}} \times 100 \quad (1)$$

$$Y_{PW}(\%) = \frac{TS_{PW} \times V_{PW}}{W_{Feedstock}} \times 100 \quad (2)$$

HHV of the dried solid samples was determined using the Schuster equation (Schuster et al., 2001) (Eq. (3), which considers C, H, N, S, O, and ash content (in wt%):

$$\mathrm{HHV}\left(\mathrm{MJ\,kg^{-1}}\right) = 0.3491 \times \mathrm{C} + 1.033 \times \mathrm{H} + 0.1005 \times \mathrm{S} - 0.0151 \times \mathrm{N} - 0.103 \times \mathrm{O} - 0.0211 \times \mathrm{Ash} \quad (3)$$

The specific methane production (SMP) (Nm^3 CH_4 kg^{-1} TCOD) obtained from the anaerobic tests was converted into HHV_{PW} using Eq. (4).

$$HHV_{PW}\left(MJkg^{-1}\right) = 39.8 \times SMP \times \frac{TCOD}{TS} \quad (4)$$

where 39.8 is the lower heating value for pure methane (MJ Nm^{-3}), and TCOD to TS ratio (kg TCOD kg^{-1} TS) is calculated from the PW.

The energy yield (E_{yield}) was calculated as the ratio between the higher calorific value of hydrochar (HHV_{HC}) and that corresponding to the feedstocks (SM and GPW) taking into account the amount added (X_{SM} and X_{GPW}) on a dry basis (Eq. (5).

$$E_{yield}(\%) = \frac{Y_{HC} \times HHV_{HC}}{HHV_{SM} \times X_{SM} + HHV_{GPW} \times X_{GPW}} \times 100 \quad (5)$$

The energy recovery from HTC products (hydrochar and methane)

Table 2
Main characteristics of hydrochars from HTC of SM and GPW, and co-HTC of both waste (SM:GPW) in dry basis (wt.%).

	HC-SM	HC-3:1	HC-1:1	HC-1:3	HC-GPW
Y_{HC} (%)	55.3 (1.4)^a	47.5 (1.2)^c	53.2 (1.0)^a	71.7 (0.5)^d	87.6 (1.3)^b
VM (%)	53.9 (0.2)^a	69.3 (0.1)^b	67.8 (0.1)^b	71.9 (0.2)^c	67.1 (0.2)^b
FC (%)	14.5 (0.1)^a	15.6 (0.1)^a	18.7 (0.1)^c	19.1 (0.2)^c	29.6 (0.2)^b
Ash (%)	31.6 (0.1)^a	15.1 (0.1)^c	13.5 (0.1)^c	9.0 (0.1)^d	3.3 (0.1)^b
C (%)	37.5 (0.3)^a	43.3 (0.2)^c	45.0 (0.4)^c	48.2 (0.5)^b	49.8 (0.3)^b
H (%)	4.7 (0.2)^a	5.1 (0.2)^b	5.5 (0.2)^c	5.1 (0.2)^b	5.3 (0.2)^b
N (%)	2.4 (0.0)^a	1.8 (0.1)^c	1.8 (0.1)^c	2.3 (0.0)^a	1.3 (0.1)^b
S (%)	0.7 (0.1)^a	0.3 (0.0)^b	0.3 (0.0)^b	0.2 (0.0)^b	0.2 (0.0)^b
O (%)	23.1 (0.3)	34.4 (0.1)	33.9 (0.2)	35.2 (0.2)	40.1 (0.2)
HHV (MJ kg^{-1})	14.9 (0.4)^a	17.0 (0.2)^c	18.1 (0.6)^b	18.5 (0.6)^b	18.7 (0.3)^b
E_{yield} (%)	61.0 (0.3)^a	55.1 (0.3)^a	58.8 (0.2)^a	77.4 (0.3)^c	89.2 (0.4)^b

Oxygen (O) content were calculated by difference (O = 100 − C − H − N − S–ash (%)).

was calculated by Eq. (6).

$$E_{recovered}\left(MJkg^{-1}\right) = HHV_{HC} \times Y_{HC} + HHV_{PW} \times Y_{PW} \quad (6)$$

2.7. Statistical analysis

Characterization tests of hydrochar and process water were performed in triplicate and were statistically analyzed by Analysis of variance (ANOVA) using the Origin 8.1 software. The minimum significant Fisher difference (Fisher LSD) was calculated with a confidence level of 0.05. In order to determine significant differences between treatments, multiple comparisons were analyzed. Also, the cumulative methane yield and SCOD removal from AD tests were analyzed by ANOVA.

3. Results

3.1. Hydrochar and process water characteristics

SM is a waste characterized by a high ash (24 wt%), N (2.9 wt%) and S (0.7 wt%) content, while GPW by a high C (47 wt%) content and HHV (20 MJ kg^{-1}) (Table 1). Table 2 shows the main characteristics of the hydrochar obtained by HTC from SM and GPW and co-HTC from these wastes. Hydrothermal treatment of both wastes separately resulted in widely different Y_{HC} values (~55% and ~ 88% for HC-SM and HC-GPW, respectively). Furthermore, 32 wt% of the hydrochar corresponds to ash for HC-SM, while only 3.5 wt% was ash for HC-GPW. Feedstock composition plays a key role in hydrochar yield and characteristics. SM is mainly composed of proteins, fats, and carbohydrates (Cao et al., 2011), therefore, a significant amount of the organic matter was transferred to the process water by hydrolysis, dehydration, and decarboxylation reactions. However, lignocellulosic biomass is composed of hemicellulose, cellulose and lignin that require high temperatures for hydrolysis (Volpe et al., 2020). Due to the reaction temperature used (180 °C), only hemicellulose is partially hydrolyzed, showing a high Y_{HC} value. Co-HTC of SM and GPW at different mass ratios (3:1, 1:1 and 1:3) significantly improved the quality of hydrochar as biofuel compared to HC-SM. The hydrochars presented values of VM and FC content in the range 68 – 72 wt% and 14 – 19 wt%, respectively, with a significant reduction in ash content ($p > 0.05$) with respect to HC-SM. Hydrochars showed a significant increase in C content ($p > 0.05$), and HHV (15 – 28%), as well as lower N and S content. These results indicate a positive synergistic effect of co-HTC of SM and GPW that allows to improve the quality of hydrochar as solid biofuel, allowing to fulfill the ISO/TS 17225–8 standard for HC-1:3 (N < 3 wt%; S < 0.2 wt%; HHV > 17 MJ kg^{-1}; and ash < 10 wt%), with a slightly decrease in Y_{HC} and E_{yield} with respect to HC-GPW.

The co-HTC of SM and GPW significantly improved the characteristics of the hydrochar as the GPW ratio increased. With a GPW ratio in the blend above 50%, the resulting hydrochar complied with the requirements of ISO/TS 17225–8 to be used as a biofuel. Similar results were obtained in co-HTC of cow dung with grape pomace and corn stover (Mariuzza et al., 2022) and in co-HTC of SM with different lignocellulosic residues (sawdust and corn stalk) (Lang et al., 2018), where increasing the proportion of lignocellulosic biomass gradually improved the quality of hydrochars to be used as solid biofuel. The co-HTC with high lignocellulosic biomass proportion decreases the retention of mineral and heavy metals in the hydrochar structure promoting the use of hydrochar as a biofuel or organic soil amendment. A hydrochar with low ash content reduces the likelihood of slagging and fouling in combustion boilers, while also improving heat transfer (Brown et al., 2020), whereas a low content of heavy metals in hydrochar used as a soil amendment reduces the soil toxicity (Alloway et al., 2021). Besides, this fact together with the acidification of the process by the addition of lignocellulosic biomass and the hydrolysis of less thermally stable compounds in short-chain acids lead the migration of phosphorus to the liquid fraction making attractive as substrate for mineralizing those dissolved ions as phosphorus-rich salts.

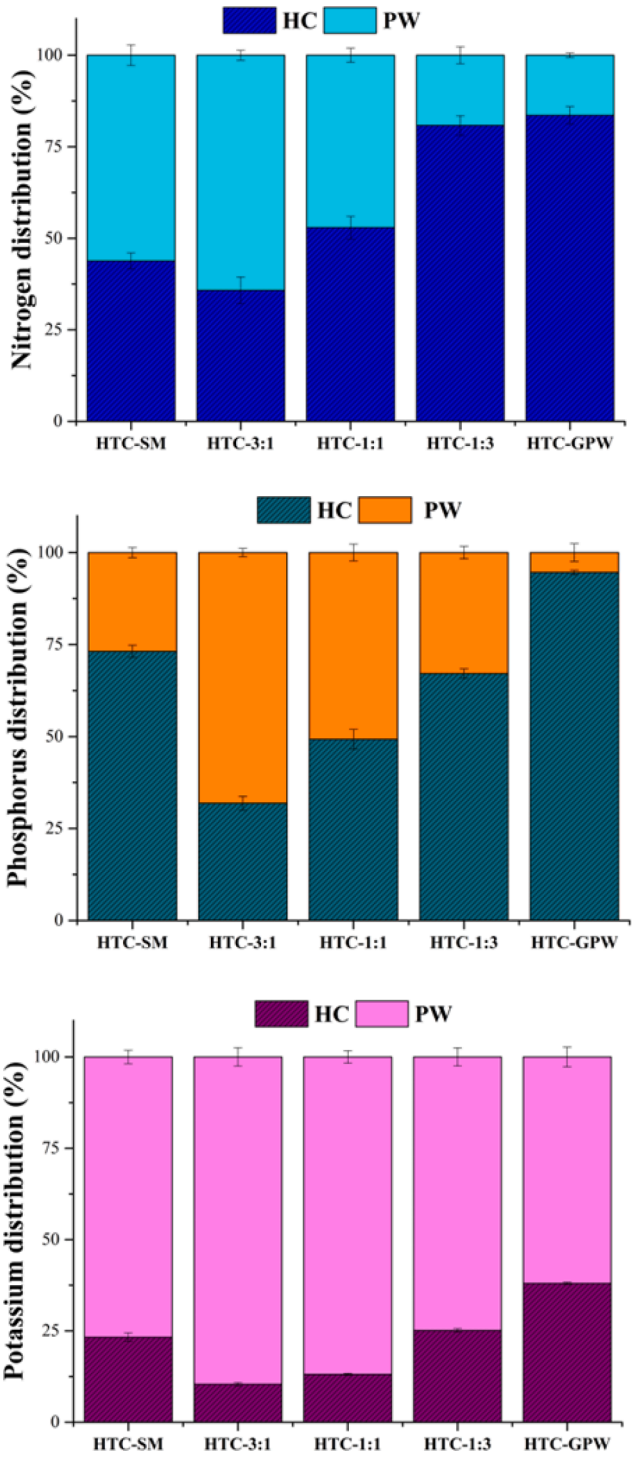

Fig. 1. Nutrient fate in HTC and co-HTC of SM and GPW.

The fate of the nutrients (N, P, and K) is interesting considering the potential use of hydrochar or process water as a soil amendment (Suarez et al., 2023) or liquid fertilizer (Belete et al., 2021), respectively. Fig. 1 shows the fate of nutrients in the HTC and co-HTC assays. Due to the low nutrient content in the GPW, the HTC of GPW showed a negligible nutrient release into the process water (2.1 g N $kg_{Feedstock}^{-1}$, 0.2 g P $kg_{Feedstock}^{-1}$, and 0.6 g K $kg_{Feedstock}^{-1}$), meaning that 16% of N, 6% of P, and 42% of K from the GPW were solubilized in the aqueous phase. HTC of SM allowed retaining a considerable amount of nutrients in hydrochar (10.5 g N $kg_{Feedstock}^{-1}$, 22.5 g P $kg_{Feedstock}^{-1}$ and 8.2 g K $kg_{Feedstock}^{-1}$),

accounting around 44% N, 73% P and 24% K, respectively. In the co-HTC assays, as the ratio of GPW in the mixture increased, due to the rigid structure of the lignocellulosic biomass and the moderate HTC temperature, the hydrolysis of N compounds was negligible, so that N remained mostly in the solid fraction. The N content of the liquid phase corresponded mainly to organic N (N-Org, 50 – 80 wt%) (see Table 3). Although the GPW shows negligible P content (~1 g $kg_{F\ eedstock}^{-1}$), co-HTC with SM at low concentrations allowed high P leaching into the process water (16 g P $kg_{F\ eedstock}^{-1}$) in co-HTC-3:1, decreasing to around half (8.5 g P $kg_{F\ eedstock}^{-1}$) in co-HTC-1:3, a value similar to that obtained in HTC-SM (8.2 g P $kg_{F\ eedstock}^{-1}$). These results could be attributed to the low content of polyvalent metals in GPW, such as Ca, Mg, Al, and Fe, that could prevent the formation of insoluble phosphorus salts (Ovsyannikova et al., 2019). As the GPW content in the feedstock increased, the content of metals, such as Ca, Mg, Al, and Fe decreased significantly, resulting in a lower concentration of ions of these metals in the process water, which does not allow reaching the stoichiometric ratio with respect to PO_4^{3-} to form insoluble salts that precipitate in the hydrochar (Sarrion et al., 2022). In the case of HTC-SM, because of the high content of polyvalent metals in SM, the formation of insoluble complex salts precipitating in the hydrochar structure could be possible (Sarrion et al., 2021). Potassium was mostly solubilized in the process water (3 – 7 g K $kg_{F\ eedstock}^{-1}$) after the HTC and co-HTC processes, due to its high solubility (Jensen et al., 2001),

Table S1 shows the mineral and heavy metal content of hydrochars obtained by HTC and co-HTC from SM and GPW. The hydrochar from SM contains a high mineral and heavy metal content compared to that from GPW, as corresponds with the composition of both raw materials (Table 1). In general, the content of monovalent metals (Na and K) decreases in the hydrochars with respect to the raw materials, due to their high solubility (Table 1). Low Na and K content in biofuel decreases the ash melting point and consequently avoid ash agglomeration and corrosion during hydrochar combustion (Magdziarz et al., 2018). On the contrary, the content of divalent and trivalent metals in the hydrochars is clear. Thus, Ca, Mg and P accounted around 70 – 85% of the total ash content in hydrochars. The accumulation of Ca, Mg, Al, and Fe is closely associated with the immobilization of P in hydrochars, by the formation of insoluble phosphorus salts with these metals (see Fig. 1 and Table S1). In the co-HTC assays, increasing the GPW ratio reduced the content of divalent and trivalent metals in the hydrochar. The analysis of the metal content (mineral and heavy metals) is of interest for the potential use of hydrochar as a solid biofuel or soil amendment. The sequestration of nutrients, especially P and N, in hydrochar is coupled with a high immobilization of heavy metals, which increased with increasing proportion of SM.

Nutrient retention in hydrochar could be of interest for using as a soil amendment or organic fertilizer (Sharma et al., 2020). In this case, the content of heavy metal content is crucial due to regulation 1009/2009 on making available on the EU fertilizer market (European Union, 2019). On the contrary, if it is intended to recover nutrients as phosphorus-rich salts by chemical precipitation, it would be necessary to improve the migration of P to the process water (Qaramaleki et al., 2020), which consequently requires improving the solubilization of polyvalent metals and P as PO_4^{3-}.

Table 3 shows the composition of the process water from the HTC and co-HTC of SM and GPW. The process water is of potential concern as a secondary source of renewable energy because of the high content of organic matter and/or nutrients. Process water characteristics varied depending on the feedstock used and the SM:GPW ratio in the co-HTC assays. The pH values for PW-GPW and PW-1:3 were acidic (≈ 4), due to the relative high concentration of TVFA (3.2 – 3.7 g acetic acid L^{-1}) derived from the hydrolysis of organic compounds from the feedstocks, and the low content of TKN (0.8 and 2.2 g L^{-1}) and TAN (<0.5 g L^{-1}). However, neutral, or slightly basic pH was achieved for PW-SM, PW-3:1 and PW-1:1, which is consistent with the lower TVFA values (1.6 – 2.5 g L^{-1}) than those obtained for PW-GPW and PW-1:3, and higher TKN (3.0 – 3.4 g L^{-1}) and TAN (1.1 – 1.8 g L^{-1}) values, with significant effect ($p > 0.05$) with the GPW ratio. Organic matter content as TCOD (29 – 61 g L^{-1}) and TOC (10 – 36 g L^{-1}) was relatively high for all process waters. The

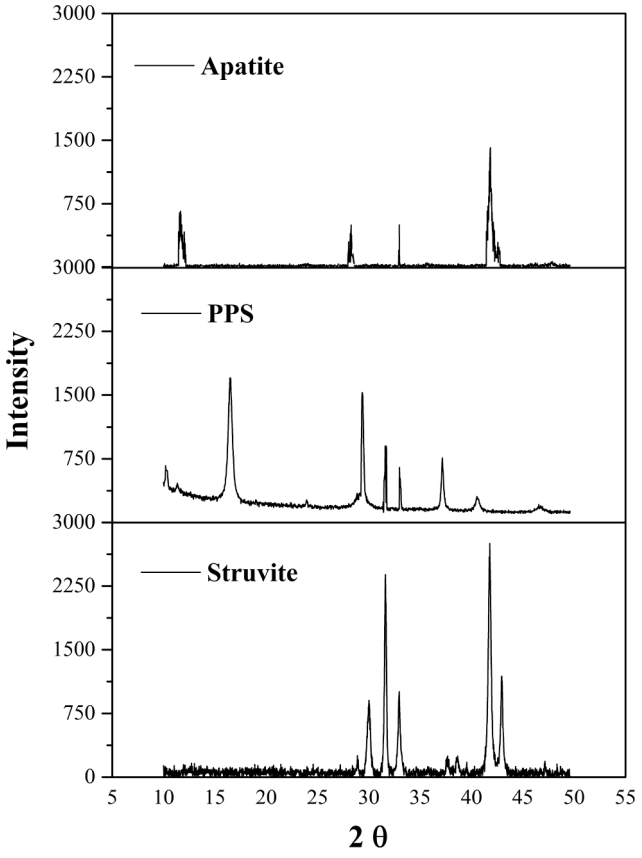

Fig. 2. XRD pattern of apatite, phosphorus precipitate salt, and struvite.

Table 3
Main characteristics of process water from HTC and co-HTC of SM and GPW.

	PW-SM	PW-3:1	PW-1:1	PW-1:3	PW-GPW
Y_{PW} (%)	36.3 (1.2)^a	33.5 (0.4)^a	27.2 (0.3)^c	19.7 (0.3)^d	11.0 (0.5)^b
pH	9.6 (0.1)^a	8.2 (0.1)^a	7.9 (0.1)	4.2 (0.1)	3.5 (0.1)
TCOD (g L^{-1})	30.5 (1.2)^a	29.1 (1.0)^a	41.1 (1.6)^c	61.3 (1.2)^d	51.1 (1.0)^b
TOC (g L^{-1})	9.6 (0.1)^a	12.9 (0.2)^a	12.6 (0.3)^a	22.8 (0.5)^c	36.4 (0.5)^b
TS (g L^{-1})	24.6 (0.2)^a	23.7 (0.4)^a	27.9 (2.1)^b	49.1 (0.3)^c	30.7 (0.5)^b
VS (g L^{-1})	16.0 (0.3)^a	19.4 (0.3)^a	22.9 (1.5)^b	37.5 (0.3)^c	26.9 (0.6)^b
TVFA (g acetic acid L^{-1})	1.8 (0.1)^a	1.6 (0.1)^a	2.5 (0.1)^c	3.2 (0.1)^b	3.7 (0.1)^b
PO_4-P (mg L^{-1})	156.0 (0.1)^a	107.0 (1.2)^c	110.5 (0.6)^c	437.0 (1.0)^d	7.7 (0.5)^b
TKN (g L^{-1})	1.7 (0.1)^a	3.4 (0.1)^c	3.0 (0.1)^c	2.2 (0.1)^d	0.8 (0.1)^b
TAN (g L^{-1})	1.1 (0.2)^a	1.8 (0.1)^c	1.8 (0.1)^c	0.5 (0.1)^b	0.2 (0.0)^b
N-Org. (g L^{-1})	0.6 (0.1)^a	1.7 (0.1)^b	1.1 (0.1)^c	1.8 (0.1)^b	0.6 (0.0)^a

VS/TS ratio reached values of 0.9 for PW-GPW, and decreased to 0.6 for PW-SM, consistent with the high presence of soluble inorganic matter. In the case of process water from co-HTC, the VS/TS ratio reached values ~ 0.8. Regarding PO_4-P content, the highest content was observed for PW-1:3 (437 mg/L). Increasing the SM:GPW ratio did not increase the PO_4-P concentration, which remained in the range 107 – 110 mg/L, values close to those obtained in PW-SM (156 mg L^{-1}).

Figure S1 shows the individual concentration of VFA expressed as acetic acid of HTC and co-HTC process waters from SM and GPW. Acetic acid (C2) accounts for around 80 – 89% of the TVFA, followed by butyric acid (C4) 2 – 9%. The SM compounds (carbohydrate, fat and proteins) does not produce TVFA, while sugar monomers are solubilized from GPW into the process water being hydrolyzed into VFA (Yang et al., 2022).

3.2. Phosphorus recovery from process water

The P migration to process water can be valorized as precipitated phosphorus salt (PPS) to be used as fertilizer. In order to obtain struvite, PW-1: 3, which presented the highest amount of PO_4^{3-}, was treated with a Mg salt to achieve a 1:1.3:1 M ratio of NH_4:Mg:PO_4. As a result, an amorphous crystalline structure, according to XRD analysis (Fig. 2) which does not resemble commercial struvite or apatite (RRUFF, 2023), was obtained. The low-quality peaks and the absence of struvite formation could be explained by the complexity of the hydrothermal carbonization process water, with a high content of organic matter and dissolved metals resulting in the formation of more than one phosphorus salt in the same structure. The process water PW-1:3 after PR, shows a reduction of organic matter (TCOD, TOC and TVFA) 30 – 40%. The PW-1:3 lossing up to 48% (1.3 g L^{-1}) of TVFA, being the reduced acetic acid about 80%. In addition, the phosphorus removal in form of PO_4^{3-} and TAN from PW-1:3 reached 95% and 60%, respectively.

PPS shows a high content of essential nutrients (Table S2), and thus they could be considered a fertilizer according to EU 1009/2019 (European Union, 2019). The N/P/K of PPS was 2.1/7.8/2.1 and reached up to 45% of the total mineral content. The heavy metal content in the PPS was negligible, except for Zn, accounting for 96% of the total, but far lower than the limit value of 800 mg Zn kg^{-1} required by EU 1009/2019. The PPS contained 7.3 wt% C, therefore it is classified as organic fertilizer (C > 3 wt%) (European Union, 2019) and its use must be limited up to 170 kg N ha^{-1} (EU nitrate directive (EU 91/676/ECC)) (Köninger et al., 2021).

3.3. Methane production from anaerobic digestion of process water

Fig. 3 shows the cumulative methane production from the anaerobic digestion of the feedstocks and process water. Ultimate methane production lower than 75 mL CH_4 g^{-1} COD_{added} for the feedstocks was observed, in agreement with their low COD removal 15% (SM) and 18% (GPW). The methane yield of PW-GPW and PW-1:3 reached values in the range 305 – 325 mL CH_4 g^{-1} COD_{added}, and remarkable COD removal of 50 – 65%, while a decreased below 210 mL CH_4 g^{-1} COD_{added} coupled with low COD removal (30 – 40%) was observed for PW-1:1, PW-SM, and PW-3:1, probably due to the presence of recalcitrant compounds. Refractory compounds are usually formed in hydrothermal treatments by Maillard reactions between sugars and amino acids, yielding compounds containing N-heteroatoms (pyrazines, pyrimidines, pyrroles), organic acids (lactic, propionic, benzoic acid), aromatic compounds (phenols, furans, benzaldehyde), among others (Ipiales et al., 2022; Marin-Batista et al., 2019; Xiao et al., 2019). COD removal and methane production showed significant decrease ($p > 0.05$) affected by SM:GPW ratio. This is related to the content of easily biodegradable and methanable compounds, in this way high acetic acid concentration (see Fig. S1) entails high removal rates and methane production.

Fig. 4 shows the energy recovery considering two different scenarios: i) direct AD of raw feedstocks, and ii) integration of HTC and AD as a strategy for the valorization of biomass waste. The HHV (14.3 MJ kg^{-1} and 19.5 MJ kg^{-1} for SM and GPW) was considered as the energy content of the feedstocks, while the total energy content in the HTC and co-HTC assays considered the HHV of hydrochars and methane yielded in AD, in both cases referred to feedstock. The AD of SM and GPW allowed a minimum energy recovery of 2.6 MJ kg^{-1} (18%) and 2.8 MJ kg^{-1} (14%) because of the low anaerobic biodegradability of raw substrates (see Fig. 3). The energy recovery with hydrochar is between 3 and 6-fold than those recovered from AD of the feedstocks. Energy recovery coupling HCT and AD can provide 10 – 18 MJ kg^{-1}, 61 – 79% comes from hydrochar. Although AD provides a lower energy recovery, process water management is compulsory to avoid the potential negative environmental impact of this HTC fraction, therefore the valorization can be positively considered (Ipiales et al., 2021). These results suggest that HTC is a suitable alternative for energy recovery from biomass waste with low biochemical methane potential.

Mass and energy balances of the potential integration of HTC, PR and AD were performed (Table 4 and Fig. S3) using the experimental data obtained in this study and the energy evaluation performed by Ipiales et al. (2022). Hydrochar is the main product of HTC and co-HTC, and reaches values of 475 – 834 kg $t_{F\ feedstock}^{-1}$ on a dry basis. The energy required in the process (energy input) was controlled by the thermal energy to heat the HTC reactor ~ 86% (see Table S3). The energy input

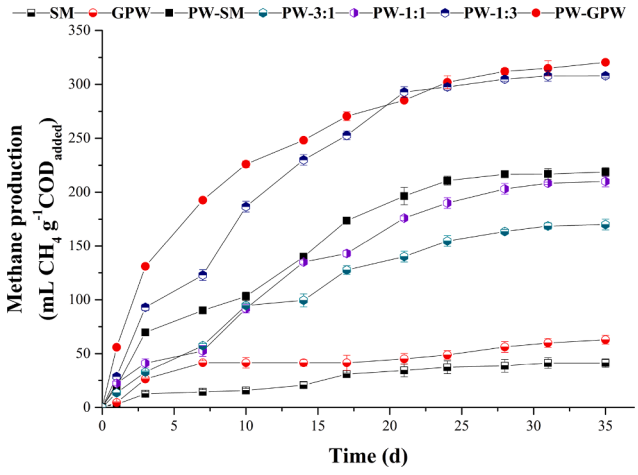

Fig. 3. Cumulative methane production from AD of SM and GPW, and process water from HTC and co-HTC of SM.

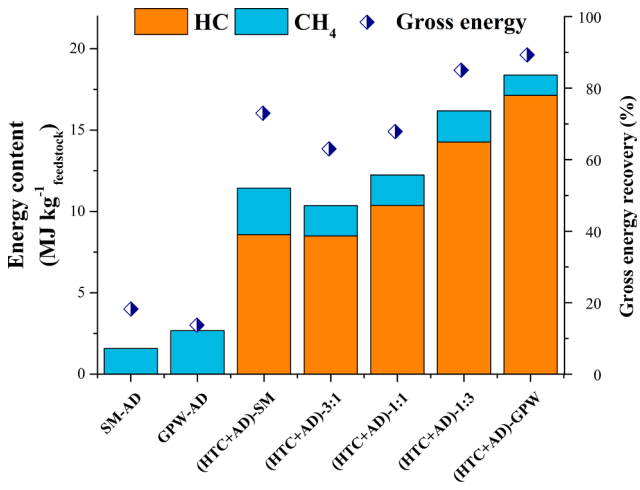

Fig. 4. Energy content and gross energy recovery by HTC and AD integration.

Table 4
Hydrochar, phosphorus-rich precipitated salts and methane production through hydrothermal carbonization, phosphorus recovery and anaerobic digestion integration on dry basis.

	Hydrochar (kg $t^{-1}_{Feedstock}$)	PPS (kg $t^{-1}_{F\ eedstock}$)	Methane (m^3 STP CH_4 $t^{-1}_{Feedstock}$)
(HTC + PR + AD)-SM	553.0	65.4	3.4
(HTC + PR + AD)-3:1	475.0	125.5	1.7
(HTC + PR + AD)-1:1	532.0	63.5	2.3
(HTC + PR + AD)-1:3	717.0	21.8	4.2
(HTC + PR + AD)-GPW	836.0	1.6	1.8

to carry out the process (2270 – 2315 kWh $t^{-1}_{F\ eedstock}$) was lower than the energy output (2500 – 4830 kWh $t^{-1}_{F\ eedstock}$) with a net energy of up to 2560 kWh $t^{-1}_{F\ eedstock}$ (HTC + AD)-GPW. The lowest net energy is obtained from (HTC-AD)-3:1 because of the low Y_{HC} (47.5%), but this has the advantage of higher phosphorus salt production (175 kg $t^{-1}_{F\ eedstock}$).

To scale the HTC process, some challenges remain, such as the related to the design of the continuous reactor and the study of phenomena related to fluid dynamics, viscosity, density, rheology, or sedimentability, being relevant the kinetic understanding of the process to predict the possible products obtained from a wide range of waste (Gallifuoco et al., 2017). Some case studies have evaluated the scale-up of the process considering the potential synergy of HTC with other technologies. Hitzl et al. (2015) operated an HTC pilot plant fed with garden pruning (1200 – 2400 kg per day) during two years in the framework of a local biorefinery, resulting in a hydrochar suitable for biofuel, phosphorous recovery from ashes, and process water valorization by crop irrigation, or as a substrate for biogas production. Lucian et al. (2021) evaluated the improving dewaterability of hydrochar obtained in the acid HTC of digested agro-industrial sludge produced in an HTC industrial-scale plant (700 L h^{-1}). Hydrochar proved to be a good candidate as a soil amendment, while the nutrients (P) were concentrated in the liquid phase (promoted by the acid addition), and recovery as microcrystalline struvite with suitable characteristics to be used as a fertilizer.

Scaling up the co-HTC process requires evaluating the implementation of local and decentralized plants near swine farms (or any industry) and close to lignocellulosic wastes, involving short transport distances from and to the plant to improve the efficiency of the process (Bevan et al., 2020). The synergy between lignocellulosic residues, with low water content, high C content and HHV and low ash (including heavy metals), N and S content, but poor in nutrients (specially P), with swine manure, a high moisture waste, rich in nutrients but poor in C or HHV, presents an alternative for swine manure valorization in terms of energy recovery and fertilizer production. Moreover, large-scale Co-HTC could produce a positive energy balance being an energetically self-sufficient process, providing environmental benefits, reducing emissions with zero CO_2 emissions and an opening to monetize swine manure, closing the HTC cycle, and moving towards a circular bioeconomy (Hitzl et al., 2015).

4. Conclusions

Hydrothermal treatment of SM yielded a low-quality hydrochar to be used as biofuel. Co-HTC of SM with GPW improved the hydrochar characteristics and HHV and allowed to increase solubilization of P and biodegradability of process water, especially with a GPW ratio higher than 50%. The precipitated phosphorus salt from the process water showed high P content and minimal heavy metal content. The AD of the process water achieved high organic matter removal and methane production. The HTC and AD integration resulted in 5- and 6-fold gross energy recovery compared with direct AD of feedstocks. The energy content of the HTC products exceeded the energy needs to carry out the process (reaction and drying of the hydrochar), resulting in an energy surplus that can be disposed of as thermal or electrical energy.

Declaration of Competing Interest

The authors declare that they have no known competing financial interests or personal relationships that could have appeared to influence the work reported in this paper.

Data availability

Data will be made available on request.

Acknowledgements

Authors greatly appreciate funding from Spain's MICINN (PID2019-108445RB-I00), MINECO (PDC2021-120755-I00 and TED2021-130287B-I00), Madrid Regional Government (Project S2018/EMT-4344), and Grupo Kerbest Company. R.P. Ipiales acknowledges the financial support from the Community of Madrid (IND2019/ AMB-17092) and Arquimea Agrotech Company.

Appendix A. Supplementary data

Supplementary data to this article can be found online at https://doi.org/10.1016/j.wasman.2023.07.018.

References

APHA Standard methods for the examination of water and wastewater American Public Health Association 21st ed. 2005 Washington, DC., USA.
ASTM, 2015. Standard test methods for proximate analysis of coal and coke by macro thermogravimetric analysis. Method D7582-15. ASTM-International, Pennsylvania. https://doi.org/10.1520/D7582-15.
Alloway, B.J., Keith, L.S., n.d.. Faroon O.M., 2021. Trace Metals and Metalloids in Soils and their Bioavailability 2021 Fifth Edition Handbook on the Toxicology of Metals. https://doi.org/10.1016/B978-0-12-822946-0.00032-5.
Bardhan, M., Novera, T.M., Tabassum, M., Azharul, I.M., Atikul, I.M., Hameed, B.H., 2021. Co-hydrothermal carbonization of different feedstocks to hydrochar as potential energy for the future world: A review. J. Clean. Prod. 298, 126734 https://doi.org/10.1016/j.jclepro.2021.126734.
Belete, Y.Z., Mau, V., Yahav Spitzer, R., Posmanik, R., Jassby, D., Iddya, A., Kassem, N., Tester, J.W., Gross, A., 2021. Hydrothermal carbonization of anaerobic digestate and manure from a dairy farm on energy recovery and the fate of nutrients. Bioresour. Technol. 333, 125164 https://doi.org/10.1016/j.biortech.2021.125164.
Benavente, V., Calabuig, E., Fullana, A., 2015. Upgrading of moist agro-industrial wastes by hydrothermal carbonization. J. Anal. Appl. Pyrolysis 113, 89–98. https://doi.org/10.1016/j.jaap.2014.11.004.
Bevan, E., Fu, J., Zheng, Y., 2020. Challenges and opportunities of hydrothermal carbonisation in the UK; Case study in chirnside. RSC Adv. 10, 31586–31610. https://doi.org/10.1039/d0ra04607h.
Brown, A.E., Adams, J.M.M., Grasham, O.R., Camargo-Valero, M.A., Ross, A.B., 2020. An assessment of different integration strategies of hydrothermal carbonisation and anaerobic digestion of water hyacinth. Energies 13 (5983), 1–26. https://doi.org/10.3390/en13225983.
Cao, X., Ro, K.S., Chappell, M., Li, Y., Mao, J., 2011. Chemical structures of swine-manure chars produced under different carbonization conditions investigated by advanced solid-state 13C nuclear magnetic resonance (NMR) spectroscopy. Energy Fuel 25, 388–397. https://doi.org/10.1021/ef101342v.
Cheng, S.Y., Tan, X., Show, P.L., Rambabu, K., Banat, F., Veeramuthu, A., Lau, B.F., Ng, E.P., Ling, T.C., 2020. Incorporating biowaste into circular bioeconomy: A critical review of current trend and scaling up feasibility. Environ. Technol. Innov. 19, 101034 https://doi.org/10.1016/j.eti.2020.101034.
De la Rubia, M.A., Villamil, J.A., Rodriguez, J.J., Borja, R., Mohedano, A.F., 2018a. Mesophilic anaerobic co-digestion of the organic fraction of municipal solid waste

with the liquid fraction from hydrothermal carbonization of sewage sludge. Waste Manag. 76, 315–322. https://doi.org/10.1016/j.wasman.2018.02.046.
De la Rubia, M.A., Villamil, J.A., Rodriguez, J.J., Mohedano, A.F., 2018b. Effect of inoculum source and initial concentration on the anaerobic digestion of the liquid fraction from hydrothermal carbonisation of sewage sludge. Renew. Energy 127, 697–704. https://doi.org/10.1016/j.renene.2018.05.002.
Diaz, E., Manzano, F.J., Villamil, J., Rodriguez, J.J., Mohedano, A.F., 2019. Low-cost activated grape seed-derived hydrochar through hydrothermal carbonization and chemical activation for sulfamethoxazole adsorption. Appl. Sci. 9 (5127), 1–14. https://doi.org/10.3390/app9235127.
EEA, 2020. Bio-waste in Europe-Turning challenges into opportunities. Copenhagen. https://doi.org/10.2800/630938.
European Union, 2019. Regulation, E. U. (2019). 1009 of the European Parliament and of the Council of 5 June 2019 Laying Down Rules on the Making Available on the Market of EU Fertilising Products and Amending Regulations (EC) No 1069/2009 and (EC) No 1107/2009 and Repealing R.
EUROSTAT, 2020. Agricultural census 2020.
Gallifuoco, A., Taglieri, L., Scimia, F., Papa, A.A., Di Giacomo, G., 2017. Hydrothermal carbonization of Biomass: New experimental procedures for improving the industrial Processes. Bioresour. Technol. 244, 160–165. https://doi.org/10.1016/j.biortech.2017.07.114.
Gao, L., Volpe, M., Lucian, M., Fiori, L., Goldfarb, J.L., 2019. Does hydrothermal carbonization as a biomass pretreatment reduce fuel segregation of coal-biomass blends during oxidation? Energy Convers. Manag. 181, 93–104. https://doi.org/10.1016/j.enconman.2018.12.009.
Hadroug, S., Jellali, S., Jeguirim, M., Kwapinska, M., Hamdi, H., Leahy, J.J., Kwapinski, W., 2021. Static and dynamic investigations on leaching/retention of nutrients from raw poultry manure biochars and amended agricultural soil. Sustain. 13, 1–26. https://doi.org/10.3390/su13031212.
Hitzl, M., Corma, A., Pomares, F., Renz, M., 2015. The hydrothermal carbonization (HTC) plant as a decentral biorefinery for wet biomass. Catal. Today 257, 154–159. https://doi.org/10.1016/j.cattod.2014.09.024.
Inkoua, S., Li, C., Shao, Y., Lin, H., Fan, M., Zhang, L., Zhang, S., Hu, X., 2023. Co-hydrothermal carbonization of fruit peel with sugars or furfural impacts structural evolution of hydrochar. Ind. Crops Prod. 193, 116221 https://doi.org/10.1016/j.indcrop.2022.116221.
Ipiales, R.P., de la Rubia, M.A., Diaz, E., Mohedano, A.F., Rodriguez, J.J., 2021. Integration of hydrothermal carbonization and anaerobic digestion for energy recovery of biomass waste: An overview. Energy Fuel 35, 17032–17050. https://doi.org/10.1021/acs.energyfuels.1c01681.
Ipiales, R.P., Mohedano, A.F., Diaz, E., de la Rubia, M.A., 2022. Energy recovery from garden and park waste by hydrothermal carbonisation and anaerobic digestion. Waste Manag. 140, 100–109. https://doi.org/10.1016/j.wasman.2022.01.003.
Ipiales, R.P., Sarrion, A., Diaz, E., Diaz-Portuondo, E., Mohedano, A.F., de la Rubia, A., 2023. Strategies to improve swine manure hydrochar: HCl-assisted hydrothermal carbonization versus hydrochar washing. Biomass Convers. Biorefinery 1–12. https://doi.org/10.1007/s13399-023-04027-w.
Jensen, P.A., Sander, B., Dam-Johansen, K., 2001. Removal of K and Cl by leaching of straw char. Biomass Bioenergy 20, 447–457. https://doi.org/10.1016/S0961-9534(01)00006-X.
Jin, H., Yan, D., Zhu, N., Zhang, S., Zheng, M., 2019. Immobilization of metal(loid)s in hydrochars produced from digested swine and dairy manures. Waste Manag. 88, 10–20. https://doi.org/10.1016/j.wasman.2019.03.027.
Kambo, H.S., Dutta, A., 2015. A comparative review of biochar and hydrochar in terms of production, physico-chemical properties and applications. Renew. Sustain. Energy Rev. 45, 359–378. https://doi.org/10.1016/j.rser.2015.01.050.
Köninger, J., Lugato, E., Panagos, P., Kochupillai, M., Orgiazzi, A., Briones, M.J.I., 2021. Manure management and soil biodiversity: Towards more sustainable food systems in the EU. Agric. Syst. 194 https://doi.org/10.1016/j.agsy.2021.103251.
Lang, Q., Guo, Y., Zheng, Q., Liu, Z., Gai, C., 2018. Co-hydrothermal carbonization of lignocellulosic biomass and swine manure: Hydrochar properties and heavy metal transformation behavior. Bioresour. Technol. 266, 242–248. https://doi.org/10.1016/j.biortech.2018.06.084.
Lang, Q., Chen, M., Guo, Y., Liu, Z., Gai, C., 2019a. Effect of hydrothermal carbonization on heavy metals in swine manure: Speciation, bioavailability and environmental risk. J. Environ. Manage. 234, 97–103. https://doi.org/10.1016/j.jenvman.2018.12.073.
Lang, Q., Zhang, B., Li, Y., Liu, Z., Jiao, W., 2019b. Formation and toxicity of polycyclic aromatic hydrocarbons during CaO assisted hydrothermal carbonization of swine manure. Waste Manag. 100, 84–90. https://doi.org/10.1016/j.wasman.2019.09.010.
Lang, Q., Zhang, B., Liu, Z., Jiao, W., Xia, Y., Chen, Z., Li, D., Ma, J., Gai, C., 2019c. Properties of hydrochars derived from swine manure by CaO assisted hydrothermal carbonization. J. Environ. Manage. 233, 440–446. https://doi.org/10.1016/J.JENVMAN.2018.12.072.
Lucian, M., Merzari, F., Gubert, M., Messineo, A., Volpe, M., 2021. Industrial-scale hydrothermal carbonization of agro-industrial digested sludge: Filterability enhancement and phosphorus recovery. Sustain. 13 https://doi.org/10.3390/su13169343.
Lynam, J.G., Reza, M.T., Yan, W., Vásquez, V.R., Coronella, C.J., 2015. Hydrothermal carbonization of various lignocellulosic biomass. Biomass Conv. Bioref. 5, 173–181. https://doi.org/10.1007/s13399-014-0137-3.
Magdziarz, A., Gajek, M., Nowak-Woźny, D., Wilk, M., 2018. Mineral phase transformation of biomass ashes–Experimental and thermochemical calculations. Renew. Energy 128, 446–459. https://doi.org/10.1016/j.renene.2017.05.057.
Marin-Batista, J.D., Villamil, J.A., Rodriguez, J.J., Mohedano, A.F., De la Rubia, M.A., 2019. Valorization of microalgal biomass by hydrothermal carbonization and anaerobic digestion. Bioresour. Technol. 274, 395–402. https://doi.org/10.1016/j.biortech.2018.11.103.
Mariuzza, D., Lin, J.C., Volpe, M., Fiori, L., Ceylan, S., Goldfarb, J.L., 2022. Impact of Co-Hydrothermal carbonization of animal and agricultural waste on hydrochars' soil amendment and solid fuel properties. Biomass Bioenergy 157, 106329. https://doi.org/10.1016/j.biombioe.2021.106329.
Ovsyannikova, E., Arauzo, P.J., Becker, G., Kruse, A., 2019. Experimental and thermodynamic studies of phosphate behavior during the hydrothermal carbonization of sewage sludge. Sci. Total Environ. 692, 147–156. https://doi.org/10.1016/j.scitotenv.2019.07.217.
Owsianiak, M., Ryberg, M.W., Renz, M., Hitzl, M., Hauschild, M.Z., 2016. Environmental performance of hydrothermal carbonization of four wet biomass waste streams at industry-relevant scales. ACS Sustain. Chem. Eng. 4, 6783–6791. https://doi.org/10.1021/acssuschemeng.6b01732.
Pecchi, M., Baratieri, M., Goldfarb, J.L., Maag, A.R., 2022. Effect of solvent and feedstock selection on primary and secondary chars produced via hydrothermal carbonization of food wastes. Bioresour. Technol. 348, 126799 https://doi.org/10.1016/j.biortech.2022.126799.
Qaramaleki, S.V., Villamil, J.A., Mohedano, A.F., Coronella, C.J., 2020. Factors affecting solubilization of phosphorus and nitrogen through hydrothermal carbonization of animal manure. ACS Sustain. Chem. Eng. 8, 12462–12470. https://doi.org/10.1021/acssuschemeng.0c03268.
Raposo, F., de la Rubia, M.A., Borja, R., Alaiz, M., 2008. Assessment of a modified and optimised method for determining chemical oxygen demand of solid substrates and solutions with high suspended solid content. Talanta 76, 448–453. https://doi.org/10.1016/j.talanta.2008.03.030.
Ro, K.S., Libra, J.A., Bae, S., Berge, N.D., Flora, J.R.V., Pecenka, R., 2019. Combustion behavior of animal-manure-based hydrochar and pyrochar. ACS Sustain. Chem. Eng. 7, 470–478. https://doi.org/10.1021/ACSSUSCHEMENG.8B03926.
RRUFF, 2023. Database of Raman sprectroscopy, X-Ray diffraction and chemistry of minerals [WWW Document].
Saba, A., McGaughy, K., Toufiq Reza, M., 2019. Techno-economic assessment of co-hydrothermal carbonization of a coal-Miscanthus blend. Energies 12 (630), 1–17. https://doi.org/10.3390/en12040630.
Sarrion, A., Diaz, E., Angeles de la Rubia, M., Mohedano, A.F., 2021. Fate of nutrients during hydrothermal treatment of food waste. Bioresour. Technol. 125954 https://doi.org/10.1016/j.biortech.2021.125954.
Sarrion, A., de la Rubia, A., Coronella, C., Mohedano, A.F., Diaz, E., 2022. Acid-mediated hydrothermal treatment of sewage sludge for nutrient recovery. Sci. Total Environ. 156494 https://doi.org/10.1016/j.scitotenv.2022.156494.
Schuster, G., Weigl, K., Hofbauer, H., 2001. Biomass steam gasification and extensive parametric modeling study. Bioresour. Technol. 77, 71–79. https://doi.org/10.1016/S0960-8524(00)00115-2.
Sharma, R., Jasrotia, K., Singh, N., Ghosh, P., Srivastava, S., Sharma, N.R., Singh, J., Kanwar, R., Kumar, A., 2020. A Comprehensive Review on Hydrothermal Carbonization of Biomass and its Applications. Chem. Africa 3, 1–19. https://doi.org/10.1007/s42250-019-00098-3.
Sharma, H.B., Panigrahi, S., Vanapalli, K.R., Cheela, V.R.S., Venna, S., Dubey, B., 2022. Study on the process wastewater reuse and valorisation during hydrothermal co-carbonization of food and yard waste. Sci. Total Environ. 806, 1–15. https://doi.org/10.1016/j.scitotenv.2021.150748.
Song, C., Yuan, W., Shan, S., Ma, Q., Zhang, H., Wang, X., Niazi, N.K., Wang, H., 2020. Changes of nutrients and potentially toxic elements during hydrothermal carbonization of pig manure. Chemosphere 243, 125331. https://doi.org/10.1016/j.chemosphere.2019.125331.
Suarez, E., Tobajas, M., Mohedano, A.F., Reguera, M., Esteban, E., de la Rubia, A., 2023. Effect of garden and park waste hydrochar and biochar in soil application: a comparative study. Biomass Convers. Biorefinery. https://doi.org/10.1007/s13399-023-04015-0.
Villamil, J.A., De la Rubia, M.A., Diaz, E., Mohedano, A.F., 2019. Technologies for wastewater sludge utilization and energy production: Hydrothermal carbonization of lignocellulosic biomass and sewage sludge. Wastewater Treatment Residues as Resources for Biorefinery Products and Biofuels. 133–153. https://doi.org/10.1016/B978-0-12-816204-0.00007-2.
Villamil, J.A., Mohedano, A.F., Rodriguez, J.J., De la Rubia, M.A., 2017. Valorisation of the liquid fraction from hydrothermal carbonisation of sewage sludge by anaerobic digestion. J. Chem. Technol. Biotechnol. 93, 450–456. https://doi.org/10.1002/jctb.5375.
Volpe, M., Messineo, A., Mäkelä, M., Barr, M.R., Volpe, R., Corrado, C., Fiori, L., 2020. Reactivity of cellulose during hydrothermal carbonization of lignocellulosic biomass. Fuel Process. Technol. 206, 106456 https://doi.org/10.1016/j.fuproc.2020.106456.
Wang, R., Lin, K., Ren, D., Peng, P., Zhao, Z., Yin, Q., Gao, P., 2022. Energy conversion performance in co-hydrothermal carbonization of sewage sludge and pinewood sawdust coupling with anaerobic digestion of the produced wastewater. Sci. Total Environ. 803, 149964 https://doi.org/10.1016/j.scitotenv.2021.149964.
Weidelener, A., Krampe, J., steinmetz, H., 2008. Phosphorrückgewinnung aus kommunalem klärschlamm als magnesium-ammonium-phosphat (MAP). Wasser und Abfall 23–26.
Weiss, F., Leip, A., 2012. Greenhouse gas emissions from the EU livestock sector: A life cycle assessment carried out with the CAPRI model. Agric. Ecosyst. Environ. 149, 124–134. https://doi.org/10.1016/j.agee.2011.12.015.

Xiao, H., Zhai, Y., Xie, J., Wang, T., Wang, B., Li, S., Li, C., 2019. Speciation and transformation of nitrogen for spirulina hydrothermal carbonization. Bioresour. Technol. 286, 121385 https://doi.org/10.1016/j.biortech.2019.121385.

Yang, G., Liu, H., Li, Y., Zhou, Q., Jin, M., Xiao, H., Yao, H., 2022. Kinetics of hydrothermal carbonization of kitchen waste based on multi-component reaction mechanism. Fuel 324. https://doi.org/10.1016/j.fuel.2022.124693.

Zhang, N., Wang, G., Zhang, J., Ning, X., Li, Y., Liang, W., Wang, C., 2020. Study on co-combustion characteristics of hydrochar and anthracite coal. J. Energy Inst. 93, 1125–1137. https://doi.org/10.1016/j.joei.2019.10.006.